High-resolution photoelectron spectrometry of autoionizing resonances between the ^3P and ^1D thresholds in atomic chlorine

J. Jiménez-Mier
Instituto de Ciencias Nucleares, Apartado Postal 70-543, UNAM, 04510 México, Distrito Federal, Mexico

S. J. Schaphorst and C. D. Caldwell
Department of Physics, University of Central Florida, Orlando, Florida 32816-2385

M. O. Krause
Oak Ridge National Laboratory, Oak Ridge, Tennessee 37831-6201
(Received 20 May 1997)

We present a measurement of the partial and differential photoionization cross sections for production of the fine-structure states of $Cl^+ \ ^3P_J$ in the region of the $3p^4\,^1Dnl$ $(l=0,2)$ autoionizing resonances. All series of resonances show distinctive behavior for the $J=2$ to $J=1$ cross-section ratio. The angular distribution parameter β was also measured for the two principal ionic states $(J=1,2)$. The behavior of β is very similar for both $J=1,2$ channels, except at the LS-forbidden nd^2S resonance series, where the $J=2$ channel shows a pronounced dip that indicates an important contribution from the parity-unfavored ϵd photoelectron waves. The widths of the $4d^2S$, $6s^2D$, and $7s^2D$ resonances were measured and the results are compared with available theoretical calculations. [S1050-2947(97)08010-4]

PACS number(s): 32.80.Fb, 32.80.Hd

I. INTRODUCTION

The study of the photoionization dynamics of open-shell atoms has constituted a major challenge for experimental and theoretical research. The extension of the calculation techniques that have been so succesful in the case of closed-shell atoms has proven to be a complicated task and there have been a limited number of experimental results that can help to guide theory. The halogens, with only one electron missing in the outermost p subshell, present the next level of complexity from the well-understood noble gases and thus are excellent test cases for understanding the behavior of open-shell atoms. Of the halogens, the chlorine atom probably has been the most thoroughly analyzed to date. There are detailed experimental results for the total photoionization cross section in the region between the ^3P and the ^1S thresholds [1,2]. The total photoionization cross section above the ^1S state and up to a photon energy of 62 eV, has also been measured at a discrete set of values of the photon energy [3]. More detailed measurements became possible with the development of a microwave discharge source coupled with an electron spectrometer, allowing angle-resolved and ionic-state-resolved experiments. This technique has now been used to study the branching ratios for production of the ^3P, ^1D, and ^1S states of the ion, and their respective angular distribution parameters β, in the region of the $3s\rightarrow np$ autoionizing resonances [4,5]. Photoelectron spectrometry was also used to measure the populations of the $^3P_{2,1,0}$ fine-structure states after photoionization of the $3p$ and $3s$ shells [6] and the $3p$ Cooper minimum was investigated in some detail [7]. Theoretical approaches include the random-phase approximation with exchange (RPAE) of Cherepkov and coworkers [8,9], single-configuration Hartree-Fock calculations of Manson *et al.* [10] and Pan and Starace [11], a multiconfiguration Hartree-Fock calculation by Fielder and Armstrong [12], the many-body perturbation theory of Brown, Carter, and Kelly [13], the configuration-interaction (CI) calculation of Hansen *et al.* [14], several R-matrix calculations [15–18], and the eigenchannel quantum-defect theory of Wang and Lu [19].

The only experimental data in the region between the $p^4\,^3P$ and $p^4\,^1D$ thresholds are the ion yield results of Ruščić and Berkowitz [1,2], which provide information about the total photoionization cross section. In that work they observed three series of autoionizing resonances converging to the ^1D state of the ion. One of the series consists of broad, asymmetric lines, while the other two are symmetric and very narrow. These lines result from the decay of the excited states $nd(^2S,^2P,^2D,^2F)$ or $ns\,^2D$, all based on a $3p^4\,^1D$ core. However, the $nd(^2S,^2F)$ series were not expected to contribute strongly to the ion signal because, under strict LS coupling, a ^2F state cannot be excited and a ^2S state cannot decay by autoionization. Therefore, the broad series was initially classified as $nd\,^2P$, the lower-energy sharp series as $ns\,^2D$, and the other narrow series as $nd\,^2D$ [1]. This assignment was modified later [2], after a comparison with similar results for bromine [20], which indicated that the broad lines were actually the superposition of the ^2D and ^2P resonances and the second series of narrow lines had to be identified as $nd\,^2S$. For this series, excitation is allowed in LS coupling and the decay is only possible by an admixture with the $nd\,^2P_{1/2}$ state induced by spin-orbit interaction. The only theoretical results that considered the effect of spin-orbit interaction are the CI calculation of Hansen *et al.* [14] and the eigenchannel R-matrix calculation of Robicheaux and Greene [16], and they both agree in this assignment for the second narrow series. Both calculations [14,16] also predict a fourth series of resonances that would correspond to

the production of the $nd\,^2F$ states. In this case spin-orbit interaction with a $nd\,^2D$ state is responsible for the excitation, while decay by autoionization is allowed in LS coupling. In a previous paper [21] we presented experimental evidence for the occurrence of these $nd\,^2F$ autoionizing resonances in Cl and Br.

The resolution used by Ruščić and Berkowitz [2] did not allow them to determine the widths of the narrow $ns\,^2D$ and $nd\,^2S$ resonances. However, they endeavored to put an upper limit for the width of the $6s\,^2D$ and $4d\,^2S$ resonances. The CI calculation [14] gives widths that are a factor of 10 larger than the experimental upper limit and the discrepancy is even larger for the RPAE calculation [9]. Thus far, the R-matrix calculation of Robicheaux and Greene [16], which includes spin-orbit interactions, is the only one that predicts widths that are smaller than the limit set by experiment.

In this work we present a high-resolution, angular-resolved photoelectron spectrometric study of all five series of autoionizing resonances between the ^3P and ^1D thresholds in atomic chlorine. This emission technique provides much greater detail than absorption by its ability to differentiate the partial channels and provide angular distribution parameters. Indeed, our electron energy resolution was good enough to allow a separate determination of the relative cross sections for production of the two principal fine-structure states of the ion $^3P_2$ and $^3P_1$ across the entire energy region, all well as the angular distribution parameter β of the $^3P_{2,1}$ channels. We could also determine the contribution of the $^3P_0$ ionic state at several values of the photon energy. Finally, we took advantage of the photon energy resolution [22] of the 4-m normal incidence monochromator (NIM) beam line at the Synchrotron Radiation Center in Wisconsin to measure the widths of the $4d\,^2S$, $6s\,^2D$, and $7s\,^2D$ resonances. The results are compared with the eigenchannel R-matrix calculation of Robicheaux and Greene [16].

II. EXPERIMENT

The experiment took place at the University of Wisconsin Synchrotron Radiation Center (SRC). Details of the experimental setup used to perform electron spectrometric studies of species produced in microwave discharges are given elsewhere [4,5]. The photoelectrons are analyzed in a set of three spherical sector analyzers mounted at right angles with respect to each other on a rotatable platform perpendicular to the direction of the photon beam. Partial cross sections can be obtained by setting two of the analyzers at the pseudomagic angle of $\theta_m = \frac{1}{2}\cos^{-1}(-1/3p)$, where p is the polarization of the ionizing radiation. The angular distribution parameter β can be obtained from the ratio of photoelectron intensities at 0° and 90° $R = I(0°)/I(90°)$ through the relation

$$\beta = \frac{4(R-1)}{3p(R+1)-(R-1)}. \tag{1}$$

The radiation polarization p was measured with calibrant gases at a photon energy of 21.2 eV, and was assumed to stay constant at lower energies. Photoelectron spectra were recorded in the constant pass energy mode by applying a staircase voltage to the source cell. With a nominal analyzer resolution of 42 meV, a photoelectron energy resolution of 53 meV was achieved, which includes the effect of the monochromator bandpass and shifts in the surface potentials of the source cell due to the presence of the chlorine atoms. This electron energy resolution was sufficient to resolve the $^3P_2$ peak from the group formed by the $^3P_1$ and the $^3P_0$ peaks. Constant ionic state (CIS) spectra were recorded by simultaneously scanning the photon energy and the accelerating voltage applied to the source cell in such a way that the pass energy of the analyzers always coincided with the central energy of the photoelectron peak. The relative intensities of two channels could be monitored by setting the pass energy of two of the analyzers to correspond to the energy of the respective photoelectron peaks. In this way we could simultaneously follow the behavior of the $^3P_2$ and $^3P_1$ channels.

The chlorine atoms were produced by dissociation of Cl_2 in a microwave discharge buffered with argon. The discharge tube was coated with H_3PO_4 to prevent recombination on the walls. The atoms traversed a 30-cm-long flow tube coated with halocarbon wax before entering the interaction region. Under typical conditions, 50 W of microwave power were fed into the gas mixture, with less than 1 W reflected. The pressure in the tube was held at about 100 mTorr (thermocouple reading), with an argon-to-chlorine pressure ratio of 2:3.

The ionizing radiation was provided by a bending magnet in conjunction with a 4-m NIM. The photon energy was calibrated by the position of the $7d$, $9s'$, $8d$, and $10s'$ resonances in Kr and the $15s'$ and $16s'$ resonances in Xe, which are conveniently located at both ends of the region of interest [23]. We estimate that the photon energy obtained in this fashion is accurate within 0.5 meV and the values obtained for the positions of the narrow chlorine $ns\,^2D$ and $nd\,^2S$ resonances agree, within the experimental error, with the values reported by Ruščić and Berkowitz [2]. The data were recorded in two separate runs with different 3600 l/mm gold-coated gratings. In the first the wavelength resolution was limited to about 3.0 pm, with a polarization of 0.73. With the second grating the resolution could reach 1.8 pm with a polarization of 0.80. A constant wavelength resolution of 21 pm was used in the scans across the entire energy region and a resolution between 3.5 and 1.8 pm was used to obtain the widths of the sharp resonances.

The monochromator bandpass was calibrated by two separate means. In the first the width of the $16s'$ resonance in Xe was measured and the natural width $\Gamma = 0.085$ meV [24] was removed, assuming that the convolution of the monochromator transmission function and the resonance profile is a Voigt function [25]. In the second procedure, the chlorine signal was used for calibration. We took the measured widths of the $6s$, $7s$, and $8s$ resonances as a starting value for the instrumental width in a fitting procedure [26], with the signal from the broad nd resonances treated as a straight-line background. We then varied the instrument width until a minimum in the χ^2 was found. Both procedures gave the same results, within the experimental error.

III. RESULTS

A typical photoelectron spectrum recorded with a photon energy of 21.75 eV is shown in Fig. 1. The signal from argon photoionization is the strongest and has been divided by a factor of 5 for clarity. This spectrum illustrates the electron

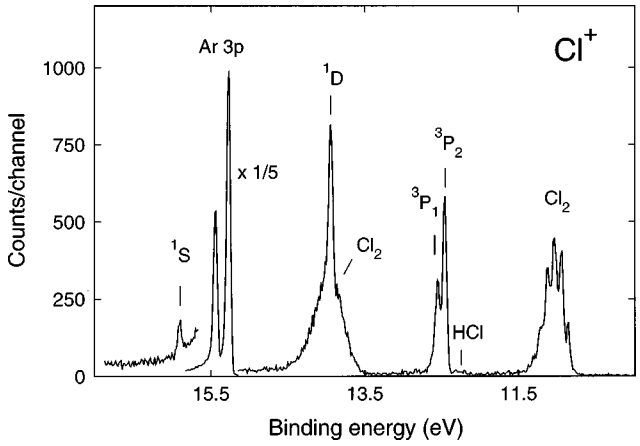

FIG. 1. Photoelectron spectrum of atomic chlorine recorded with a photon energy of 21.75 eV and at 0° with respect to the major axis of the ionizing radiation polarization. The atomic chlorine peaks are labeled according to the final state of the ion. The spectrum contains 512 points.

energy resolution that can be achieved with our spectrometer for this type of experiment. Four atomic peaks, corresponding to the production of the $^3P_2$, $^3P_{1,0}$, ^1D, and ^1S states of Cl^+ can be easily identified. The photoelectron peaks of interest in this work, namely $^3P_2$ and $^3P_1$, are readily resolved. The peak corresponding to the production of the $^3P_0$ appears as a shoulder to the higher-energy side of this apparent doublet and its intensity can be extracted by a deconvolution procedure [6]. Also, it is important to remark that there is little indication (less than 5%) of photoelectron peaks resulting from photoionization of atomic chlorine in the $^2P_{1/2}$ excited state and that there is no molecular structure due to Cl_2 in this binding-energy region. The only molecular peaks in this region correspond to HCl, and they appear as a small hump to the low-binding-energy side of $Cl^+(^3P_2)$ peaks. At the beginning of the operation of the discharge, these HCl peaks are much stronger due to the reaction of the chlorine atoms with the moisture in the coating of the tube walls, but they decrease in intensity after about 1 h of operation and continue to stay at a very low level. During the experimental runs reported in this work, the intensity of the $X^2\Pi(0\leftarrow 0)$ peaks of HCl was always less than 7.5% and typically 2% of the $^3P_2$ atomic signal. As a result, the 0.2% intensity of the $X^2\Pi(1\leftarrow 0)$ peaks near 13.1 eV, which overlap slightly with the $^3P_{2,1,0}$ structure, was entirely negligible.

The CIS spectra recorded at the pseudomagic angle across the entire energy region with a resolution of 21 pm are shown in Fig. 2. All spectra are corrected for background and for the change in the monochromator transmission as a function of the photon energy and thus are proportional to the partial cross sections. The lower panel [Fig. 2(a)] corresponds to the production of the $^3P_2$ ionic state. The behavior of the $^3P_1\epsilon l$ channel is given in Fig. 2(b)]. The intensities of Figs. 2(a) and 2(b) are normalized so that the intensity ratio between these two channels corresponds to the ratio obtained from photoelectron spectroscopy (PES) spectra recorded at selected values of the photon energy and the absolute scale gives a good indication of the actual counts in the data. Since there is some overlap in the PES peaks, there is a small contribution of Fig. 2(a) into Fig. 2(b) and vice versa.

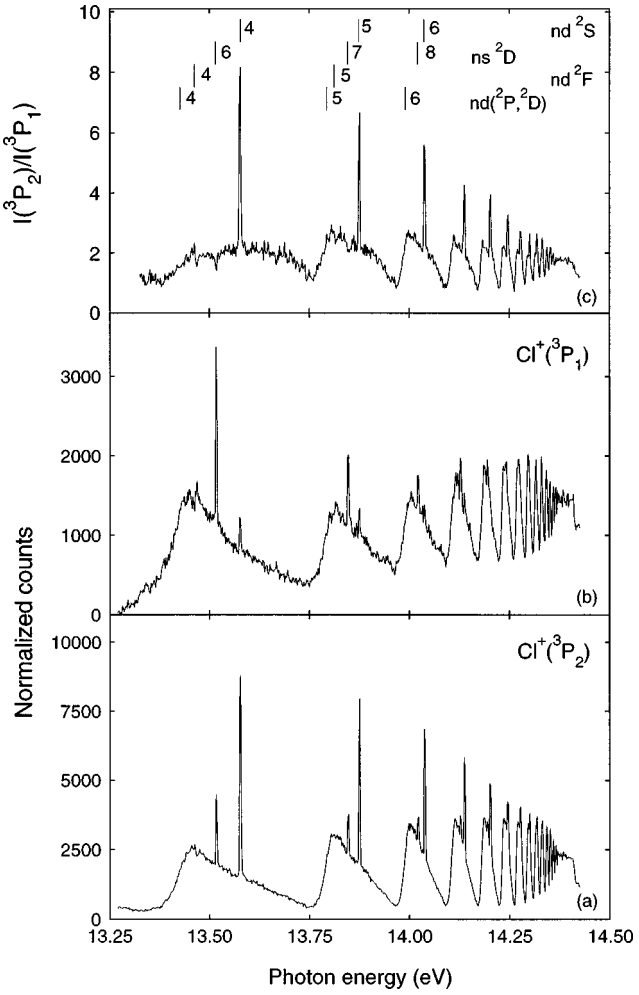

FIG. 2. Relative photoionization cross sections for production of the fine-structure states of Cl^+ across the autoionizing resonances converging toward the ^1D limit. The resonance assignment is given on top of panel (c). (a) Relative cross section for production of the $^3P_2$ state. (b) Relative cross section for production of the $^3P_1$ state. (c) Panel (a) divided by panel (b) to obtain the $I(^3P_2)/I(^3P_1)$ ratio.

We estimate that this contribution is less than 4%, and does not alter the figure significantly, except at the sharp nd^2S resonances. Finally, the ratio of Figs. 2(a) and 2(b) is presented in Fig. 2(c). Each series of resonances shows a different behavior for this intensity ratio. At the broad $nd(^2P,^2D)$ resonances the ratio goes through minima (maxima) at the intensity minima (maxima). Two dispersionlike features in the ratio correspond to the first members of the nd^2F series [21]. These resonances appear as steps in the $^3P_1$ channel in Fig. 2(b) and as dips in the $^3P_2$ signal in Fig. 2(a). The effect of the ns^2D resonances is not as pronounced and manifests itself as shallow dips in the intensity ratio. Finally, the ratio increases sharply at the peaks of the nd^2S resonances. If we subtract the contribution from the broad $nd(^2P,^2D)$ resonances we find a value for this ratio that stays almost constant and is equal to about 20. The overall behavior of the intensity ratio is similar to though less pronounced than that of the corresponding ^3P_J partial cross-section ratio in Br [21].

A set of representative photoelectron spectra recorded at the pseudomagic angle and at four different points across the

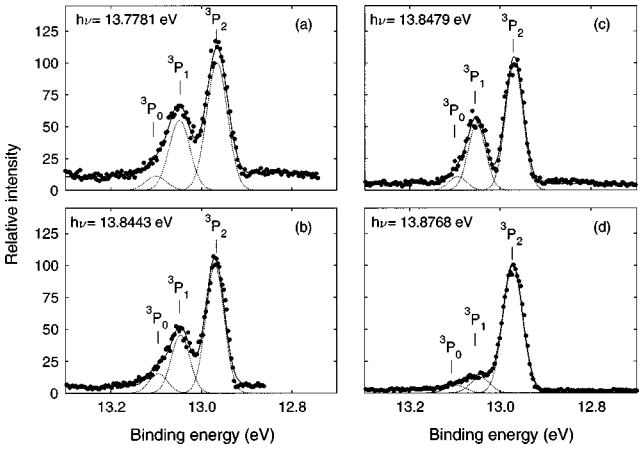

FIG. 3. Photoelectron spectra recorded at the magic angle in the region of the second group of autoionizing resonances. (a) Spectrum taken near the minimum of the broad $5d$ resonance. (b) Spectrum obtained near the top of the same resonance. (c) Spectrum recorded at the top of the $7s$ resonance. (d) Spectrum at the maximum of the $5d\,^2S$ resonance. In all the figures the dots are the experimental data, the continuous lines are the results of the corresponding overall fits, and the dotted lines are the individual fitted peaks (see the text). The electron energy resolution is 53 meV, including a monochromator bandpass of 2.3 meV.

second group of resonances is shown in Fig. 3. The electron energy resolution was 53 meV in all cases, with a monochromator bandpass of 15 pm (2.3 meV). The relative intensities of the atomic peaks were obtained by fitting three peaks of equal width and shape to the data, together with a straight-line background. The overall fit is shown as a continuous line in each of the plots and the dotted lines give the individual atomic lines with the background subtracted. The vertical scale was chosen so that the maximum of the $^3P_2$ fitted peak corresponded to a value of 100. The binding energies of the peaks agree quite well with the values given by Radziemski and Kaufman [27]. Figure 3(a) corresponds to a photon energy near the minimum of the $5d(^2P,^2D)$ resonance. As expected, the signal-to-background ratio is lowest in this spectrum, but even in this case there is only a small indication of the HCl peaks near 12.8 eV. Of the four spectra shown here, this is the one with the largest contribution from the $^3P_{1,0}$ channels. Figure 3(b) shows a spectrum recorded near the maximum of the $5d(^2P,^2D)$ resonance. Here the $^3P_0$ contribution is greater, but this might be an artifact of the fitting procedure because the sum of the $J=1,0$ channels is not too far from the respective sum in Figs. 3(a) and 3(c). Figure 3(c) was obtained at the peak of the $7s\,^2D$ resonance. The relative intensities are essentially indistingishable from those of Figs. 3(a) and 3(b). The situation is quite different at the $5d\,^2S$ resonance [Fig. 3(d)]. There is a strong enhancement of the $^3P_2$ channel with respect to the other two. It is also interesting to point out that the intensity ratio of the $J=1$ to $J=0$ channels is not very different from the values obtained at the other energies. The relative intensities of the atomic peaks in these spectra are given in Table I. For comparison, the fine-structure intensities obtained at a photon energy of 29.2 eV [6] are also given in Table I as are the geometrical branching ratios calculated by Berkowitz and Goodman [28] and by Schirmer, Cederbaum, and Kiessling [29]. Except for the results at the $5d\,^2S$ resonance, all the other values give a larger contribution from the $J=0,1$ channels compared to those measured at 29.2 eV [6] and the geometric values predicted by theory [28,29].

TABLE I. Relative intensities of the fine-structure ionic states in the photoelectron spectra.

Photon energy (eV)	Resonance	Ionic state $^3P_2$	$^3P_1$	$^3P_0$
13.7781	[a]	100	55.1(4.9)	11.3(2.0)
13.8443	[b]	100	45.7(1.3)	15.3(0.6)
13.8479	$7s\,^2D$	100	51.9(1.5)	10.7(0.5)
13.8768	$5d\,^2S$	100	9.74(.47)	2.24(.12)
29.2 [c]	none	100	40.5(1.5)	9.5(2.2)
geometric [d]		100	35.4	8.5
geometric [e]		100	36	8

[a]At trough of $5d(^2P,^2D)$ resonances.
[b]Near maximum of $5d(^2P,^2D)$ resonances.
[c]Reference [6].
[d]Reference [28].
[e]Reference [29].

The sum of the partial CIS spectra in Figs. 2(a) and 2(b) is displayed in Fig. 4(a). The curve shown can be taken to be a good indication of the *total* photoionization cross section because the contribution from the $J=0$ state, which is not included in the figure, is always less than 7% of the total in all the PES spectra. Also shown in Fig. 4 are the results for the total ionization cross section measured by Ruščić and Berkowitz [1] [Fig. 4(b)] and the results of the R-matrix calculation of Robicheaux and Greene [16] [Fig. 4(c)]. These two curves were obtained by digitizing the first three groups of resonances in Fig. 4 of Ref. [16]. Our scale was converted from energy to wavelength using the relationship $\lambda(\text{Å}) = 12\,398.424/h\nu$ (eV). The vertical scale in Fig. 4(a) was arbitrarly chosen so that the intensity at the top of the broad $5d\,^2P,^2D$ resonance in the second group is the same in Figs. 4(a) and 4(c). The ion spectrum in Fig. 4(b) was recorded with a resolution of 28 pm [1] and the theoretical results [Fig. 4(c)] were convoluted with an instrument function of the same width [16]. Our results [Fig. 4(a)] were obtained with a monochromator bandpass of 21 pm. The agreement with both the ion results and theory is quite good, even though the $ns\,^2D$ resonances in our spectrum appear smaller than in the other studies. This might be due, in part, to the fact that we are not including the contribution from the $^3P_0$ ionic channel.

The results for the angular distribution parameter β for the $^3P_2$ and the $^3P_1$ channels are presented in Fig. 5. The scans cover the second group of resonances, namely, $5d(^2P,^2D)$, $5d\,^2F$, $7s\,^2D$, and $5d\,^2S$, with a slightly better resolution of 15 pm. We also have a coarse scan between the ^3P and ^1D thresholds, with a monochromator bandpass of 21 pm, which shows that the behavior presented in Fig. 5 repeats at the other groups of resonances. In both channels the β parameter reaches the value of -1 at the minimum of the $5d(^2P,^2D)$ resonance and rises to a value close to zero at the maximum. At the $7s\,^2D$ resonance there is a feature that looks dispersionlike in the $^3P_1$ channel and appears as a shallow dip in $\beta(^3P_2)$ and $5d\,^2S$ resonances. The effect of

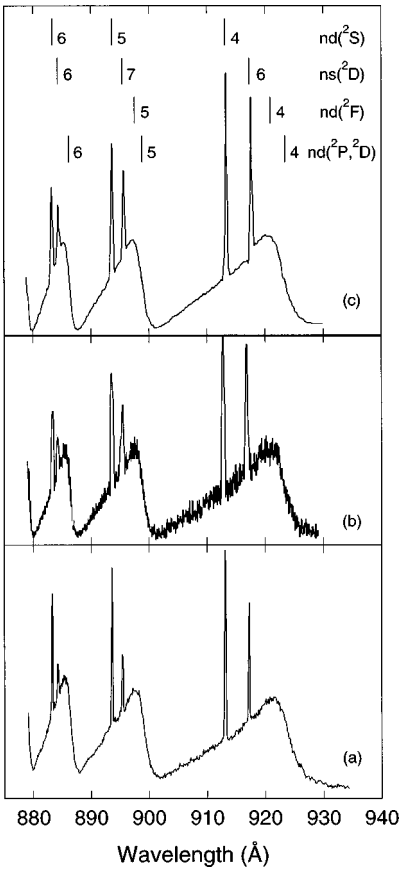

FIG. 4. Total photoionization cross section for atomic chlorine. (a) This work, representing the sum of the $^3P_2$ and $^3P_1$ cross sections shown in Fig. 2 with the horizontal scale converted to wavelength. The monochromator bandpass was 21 pm. (b) Ion yield from Ref. [1], with a resolution of 28 pm. (c) Eigenchannel R-matrix result from Ref. [16], which includes the convolution with a 28-pm window function. Note that the $^3P_0$ contribution, amounting to few percent of the total, is not included in our spectrum [panel (a)].

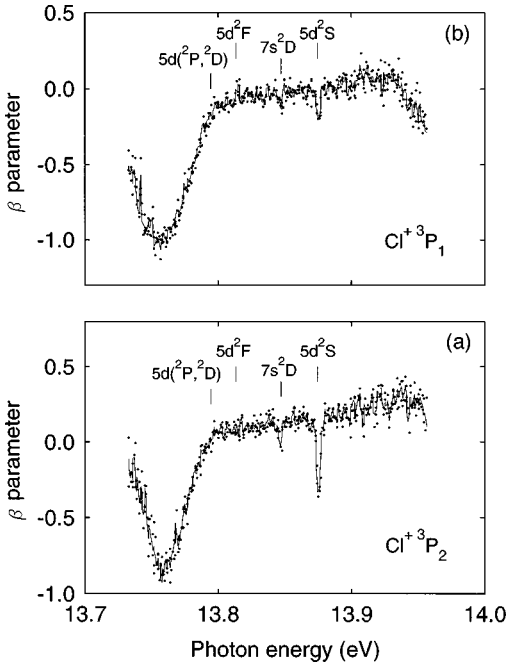

FIG. 5. Photoelectron angular distribution parameters measured over the second autoionization resonance structure. (a) β parameter for the $^3P_2$ channel. (b) β parameter for the $^3P_1$ channel. The dots are the direct experimental results and the continuous line is the result of a five-point smoothing procedure.

the $5d\,^2S$ resonance is pronounced in the $^3P_2$ channel only. The dip in $\beta(^3P_1)$ is estimated to be largely due to the contribution of the $^3P_2$ peak in the CIS spectra of the $^3P_1$ channel. Any possible contribution was not removed in any of these spectra because it would be small everywhere, less than 4% (except at the $5d^2S$ resonance), and the subtraction would considerably increase the scatter in the points. Note also that, at this level, there is no distnct effect of the $5d^2F$ resonance in the β parameter in either ionic channel.

Finally, the resolution capability of the 4-m NIM monochromator allowed us to measure the widths of the $4d\,^2S$, $6s\,^2D$, and $7s\,^2D$ resonances. A CIS spectrum recorded with a monochromator bandpass of 3.5 pm is shown in Fig. 6. This is a continuous scan that covers the entire region between the $6s\,^2D$ and the $4d\,^2S$ resonances. We also have spectra obtained at higher resolution (1.8 pm) of individual resonances. The resolution of the spectrum shown in the figure is a factor of 2 better than the resolution of Ruščić and Berkowitz [2] and our signal-to noise ratio is much superior. The data were fit to the convolution of Fano profiles and a triangular window function that simulated the Gaussian profile of the bandpass [26]. A straight-line background was used for the contribution from the broad $4d$ resonance. In the fitting procedure the monochromator bandpass was first fixed at our calibration value, until the resonance parameters were optimized. The procedure was repeated with a different bandpass, until a minimum in the χ^2 was found, which required only a very small change in the original value of the bandpass. The results for the resonance widths full width at half maximum are given in Table II. Also listed are the reduced widths Γn^{*3}, which were obtained with the effective quantum numbers n^* derived from our spectra, namely, $n^*(6s)=3.897$, $n^*(4d)=4.039$, and $n^*(7s)=4.906$. The results of the R-matrix calculation of Robicheaux and Greene [16] are also presented. A set of seven spectra were used to obtain the width of the $4d\,^2S$ resonance, five for the $6s\,^2D$ resonance, and one for $7s\,^2D$ resonance. The results

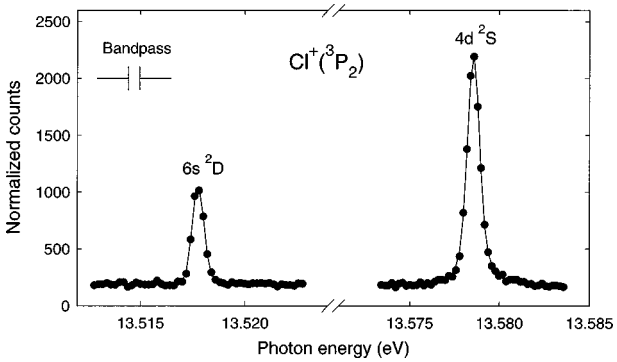

FIG. 6. Constant ionic state spectrum of the $6s\,^2D$ and $4d\,^2S$ resonances as seen in the $^3P_2$ ionic channel. Dots, experimental points; solid line, fit. The monochromator bandpass indicated corresponds to 3.5 pm or 0.5 meV.

TABLE II. Resonance widths.

	Γ (meV)		
Resonance	This work	Theory [a]	Γn^{*3} (meV)
$4d\,^2S$	0.484 (24)	0.297	31.9(1.6)
$6s\,^2D$	0.209 (24)	0.103	12.4(1.4)
$7s\,^2D$	0.13 (4)		15.4(4.9)

[a]Reference [16].

were very consistent within each set. The $4\,^2S$ resonance width is comparable to the monochromator bandpass used, while the measured widths of the $ns\,^2D$ resonances are always smaller. Thus the widths of the $ns\,^2D$ resonances become less and less accurate for the higher members. Our results for $4d\,^2S$ and $6s\,^2D$ are a factor of 2 larger than the values calculated by Robicheaux and Greene [16]. The calculations [13,9,16,17] predict an asymmetric profile for the $ns\,^2D$ resonances, which is at variance with our observation. There is no indication in any of the spectra of a minimum or tail to either side of the $ns\,^2D$ peaks. In all cases the Fano q parameter appears to be large and positive.

IV. DISCUSSION

The results presented here indicate that any theoretical approach to the treatment of photoionization dynamics in atomic chlorine must include the influence of spin-orbit interaction in order to reproduce the behavior of all five series of resonances. In particular, a calculation should be able to explain the strong coupling of the $nd\,^2S$ series into the $^3P_2\epsilon d$ continuum channel and the coupling mechanisms of the $nd\,^2F$ series into the different ionic channels that translate into different shapes and strengths. The calculation should also reproduce well the results obtained for the J-resolved angular distribution parameter $\beta(^3P_J)$.

The first point is addressed by the eigenchannel R-matrix calculation of Robicheaux and Greene [16]. They found it necessary to go beyond the standard LS to jj transformation and include the spin-orbit mixing of core states with the same total angular momentum J_c. In particular, the dynamical mixing of the $p^4\,^1D_2$ and $p^4\,^3P_2$ core states allows the decay of the $nd\,^2S_{1/2}$ resonances into the $^3P_2\epsilon d\,^2P_{1/2}$ continuum. Therefore, even though they do not show partial cross sections, we conclude that our results are in agreement with this calculation.

We also agree with the eigenchannel R-matrix calculation [16] in the sense that there is no indication for the $nd\,^2F$ series in the total cross section for chlorine (Fig. 4). However, we showed here that there is a distinctive effect in the partial cross sections. The resonances show up as window features in the $^3P_2$ channel and as dispersionlike patterns in the $^3P_1$ channel (Fig. 2). A similar behavior was found for atomic bromine [21], where the effect of this series appears even in the total cross section. Therefore, it is necessary to have a calculation at the level of partial cross sections to be able to compare with theory.

Finally, we can say a few words about our results for the angular distribution parameters. Once again, to the best of our knowledge, there is no calculation of the differential cross sections. A detailed analysis is complicated by the fact that there are many open channels and many values of the total angular momentum. Even within the framework of the angular momentum transfer formalism [30] there are many channels that have to be considered. There are three values of angular momentum transfer, $j_t=1,2,3$, all of which can originate from any of the allowed values of the total angular momentum. The fact that the main excursions in our β values are towards negative values stresses the importance of the negative terms in the expression for β, which are the parity-unfavored $j_t=2$ term associated with d-wave photoelectrons and the interference s-d term, whose sign depends on the relative phase between the channels. Both negative terms might be responsible for the broad minimum in β at the low-energy portion of the $nd(^2P,\,^2D)$ series. However, we already know that the $nd\,^2S$ series is coupled to the $^3P_2\epsilon d$ channel only. Therefore, the negative excursion at this series is due to the predominance of the parity-unfavored term in β.

V. CONCLUSIONS

We used photoelectron spectrometry to perform a high-resolution study of the photoionization of atomic chlorine between the ^3P and ^1D thresholds. We were able to follow the effect of five series of autoionizing resonances on the relative cross sections and angular distribution parameters for two of the three ionic channels ($J=2,1$). The ability to resolve the ^3P_J ionic states played a critical role in all the measurements. The results for the total ionization cross section are in good agreement with the ion measurements of Ruščić and Berkowitz [1,2] and the eigenchannel R-matrix calculation of Robicheaux and Greene [16]. Our results for the $I(^3P_2)/I(^3P_1)$ branching ratio indicate that the $nd\,^2S$ is predominantly coupled to the $^3P_2\epsilon d$ continuum, in agreement with the eigenchannel R-matrix calculation of Robicheaux and Greene [16].

The $nd\,^2F$ resonance series appears distinctively in the signal of each of the exit channels measured. Our results for the angular distribution parameters indicate an important contribution of the parity-unfavored term associated with the emission of d-wave photoelectrons. We measured the widths of some of the sharp resonances and the results are a factor of 2 higher than the values calculated by Robicheaux and Greene [16]. Further work is needed to measure the shape and width of the $nd\,^2F$ resonances. We hope that this set of experimental results will motivate calculations at the level of partial and differential cross sections, which will help in the interpretation of the photoionization dynamics of the chlorine atom.

ACKNOWLEDGMENTS

This work was supported by the National Science Foundation under Grants Nos. PHY-9207634 and PHY-9507573. M.O.K. was supported by the U.S. Department of Energy under Contract No. DE-AC05-84-OR21400 with Martin Marietta Energy Systems, Inc. The University of Wisconsin SRC is operated under National Science Foundation Grant No. DMR-9531009. J.J.M. would like to thank the Department of Physics, Tulane University, for its hospitality during the final stages of the manuscript preparation.

[1] B. Ruščić and J. Berkowitz, Phys. Rev. Lett. **50**, 675 (1983).
[2] B. Ruščić and J. Berkowitz, Phys. Rev. A **40**, 6716 (1989).
[3] J. A. R. Samson, J. Shefer, and G. C. Angel, Phys. Rev. Lett. **56**, 2020 (1986).
[4] P. van der Meulen, M. O. Krause, C. D. Caldwell, S. B. Whitfield, and C. A. de Lange, J. Phys. B **24**, L573 (1991).
[5] P. van der Meulen, M. O. Krause, C. D. Caldwell, S. B. Whitfield, and C. A. de Lange, Phys. Rev. A **46**, 2468 (1992).
[6] M. O. Krause, C. D. Caldwell, S. B. Whitfield, C. A. de Lange, and P. van der Meulen, Phys. Rev. A **47**, 3015 (1993).
[7] M. O. Krause, C. D. Caldwell, S. B. Whitfield, P. van der Meulen, and C. A. de Lange, Bull. Am. Phys. Soc. **37**, 1076 (1992).
[8] N. A. Cherepkov and L. V. Chernysheva, Phys. Lett. **60A**, 103 (1977).
[9] V. F. Orlov, N. A. Cherepkov, and L. V. Chernysheva, Opt. Spektrosk. **64**, 683 (1988) [Opt. Spectrosc. **64**, 409 (1988)].
[10] S. T. Manson, A. Msezane, A. F. Starace, and S. Shahabi, Phys. Rev. A **20**, 1005 (1979).
[11] C. Pan and A. F. Starace, Phys. Rev. A **47**, 295 (1993).
[12] W. R. Fielder and L. Armstrong, Phys. Rev. A **28**, 218 (1983).
[13] E. R. Brown, S. L. Carter, and H. P. Kelly, Phys. Rev. A **21**, 1237 (1980).
[14] J. E. Hansen, R. D. Cowan, S. L. Carter, and H. P. Kelly, Phys. Rev. A **30**, 1540 (1984).
[15] M. Lamoureaux and F. Combet Farnoux, J. Phys. (France) **40**, 545 (1979).
[16] F. Robicheaux and C. H. Greene, Phys. Rev. A **46**, 3821 (1992).
[17] S. S. Tayal, Phys. Rev. A **47**, 182 (1993).
[18] F. Robicheaux and C. H. Greene, Phys. Rev. A **47**, 1066 (1993).
[19] Z.-w. Wang and K. T. Lu, Phys. Rev. A **31**, 1515 (1985).
[20] B. Ruščić, J. P. Greene, and J. Berkowitz, Phys. Rev. B **17**, 1503 (1984).
[21] S. Benzaid, A. Menzel, J. Jiménez-Mier, S. J. Schaphorst, M. O. Krause, and C. D. Caldwell, Phys. Rev. A **54**, R2537 (1996).
[22] C. D. Caldwell and M. O. Krause, J. Phys. B **23**, 2233 (1990).
[23] K. Yoshino and D. E. Freeman, J. Opt. Soc. Am. B **2**, 1268 (1985); K. Yoshino and Y. Tanaka, J. Opt. Soc. Am. **69**, 159 (1979).
[24] This value is based on the widths of the Xe $11s'$ resonance given as 0.305 meV and 0.320 meV by M. Klar, K. Harth, J. Ganz, T. Kraft, M.-W. Ruf, H. Hotop, V. Tsemekhman, and M. Ya. Amusia, Z. Phys. D **23**, 101 (1992) and K. Maeda, K. Ueda, and K. Ito, J. Phys. B **26**, 1541 (1993), respectively, and our own value of 0.58 eV for the width of Xe $10s'$.
[25] M. O. Krause, in *Synchrotron Radiation Research*, edited by H. Winick and S. Doniach (Plenum, New York, 1980), Chap. 5.
[26] J. Jiménez-Mier, J. Quant. Spectrosc. Radiat. Transf. **51**, 741 (1994).
[27] L. J. Radziemski, Jr. and V. Kaufman, J. Opt. Soc. Am. **59**, 424 (1969); **64**, 366 (1974).
[28] J. Berkowitz and G. L. Goodman, J. Chem. Phys. **71**, 1754 (1979).
[29] J. Schirmer, L. S. Cederbaum, and J. Kiessling, Phys. Rev. A **22**, 2696 (1980).
[30] D. Dill and U. Fano, Phys. Rev. Lett. **29**, 1203 (1972).